Technical note: A new online tool for $\delta^{18}O$-temperature conversions

Daniel E. Gaskell[1], Pincelli M. Hull[1]

[1]Department of Earth & Planetary Sciences, Yale University, New Haven, CT 06511, USA

Correspondence to: Daniel E. Gaskell (daniel.gaskell@yale.edu)

Abstract. The stable oxygen isotopic composition of marine carbonates ($\delta^{18}O_c$) is one of the oldest and most widely-used paleothermometers~~, but~~. However, interpretation of these data is complicated by the necessity of knowing the $\delta^{18}O$ of the source seawater ($\delta^{18}O_w$) from which $CaCO_3$ is precipitated. The effect of local hydrography (the "salinity effect") is particularly difficult to correct for and may lead to errors of >10°C in sea-surface temperatures if neglected. A variety of methods for calculating $\delta^{18}O_w$ have been developed in the literature, but not all are readily accessible to workers. Likewise, temperature estimates are sensitive to a range of other calibration choices (such as calibration species and the inclusion or exclusion of carbonate ion effects) which can require significant effort to intercompare. We present an online tool for $\delta^{18}O$-temperature conversions which provides convenient access to a wide range of calibrations and methods from the literature. ~~Using results from recent isotope-enabled climate simulations, we show that the common method of estimating $\delta^{18}O_w$ from sample latitudes likely results in paleotemperature estimates that are too cold by up to 5°C in the North Atlantic and too hot by up to 5°C in the Southern Ocean during the warmest climate states.~~ Our tool provides a convenient way for workers to examine the effects of alternate calibration and correction procedures on their $\delta^{18}O$-based temperature estimates.

1 Motivation

The stable oxygen isotopic composition of carbonates ($\delta^{18}O_c$) is one of the oldest and most widely-used paleothermometers and undergirds a wide variety of paleoceanographic research (for recent reviews, see Pearson, 2012; Sharp, 2017). Converting $\delta^{18}O_c$ to temperature is typically done using an empirical calibration ~~such as~~in either a linear form such as

$$T = 16.5 - 4.80(\delta^{18}O_c - \delta^{18}O_w - 0.27), \quad (1)$$

(Bemis et al., 1998), or in a quadratic form such as

$$T = 16.0 - 5.17(\delta^{18}O_c - \delta^{18}O_w - 0.20) + 0.09(\delta^{18}O_c - \delta^{18}O_w - 0.20)^2, \quad (2)$$

(McCrea, 1950; as reformulated by Bemis et al., 1998), where T is temperature (in °C), $\delta^{18}O_c$ is the oxygen isotope composition of the carbonate (as ‰ VPDB), and $\delta^{18}O_w$ is the oxygen isotope composition of the water in which the carbonate was precipitated (as ‰ VSMOW). Much of the complexity of using $\delta^{18}O$ as a paleothermometer arises from the need to know $\delta^{18}O_w$, which may vary both globally as a function of ~~sea level~~ice volume and locally at the sea surface as a function of regional hydrography ~~(Sharp, 2017)~~ (Rohling, 2013). Global variation can be estimated using independent records of sea level, so the

global record of deep-water $\delta^{18}O$-based temperatures has been relatively well-established (Zachos et al., 2001; Cramer et al., 2009; Westerhold et al., 2020; Rohling et al., 2021; etc.) However, local variations in surface $\delta^{18}O_w$ are more difficult to predict, rendering sea-surface temperature (SST) estimates from $\delta^{18}O$ less reliable than deep-water temperature estimates. To address this, a variety of methods have been developed in the literature to estimate surface $\delta^{18}O_w$.

Since modern surface $\delta^{18}O_w$ broadly covaries with latitude, a common approach has been to apply the modern latitudinal variation to a sample's paleolatitude (typically using the relationship fit from Southern Ocean data in Zachos et al., 1994 Eq. 1; or more recently the updated method of Hollis et al., 2019). However, this approach performs particularly poorly in the North Atlantic and other high northern latitudes, where local $\delta^{18}O_w$ can deviate significantly from the latitudinal mean (Fig. 1; Zachos et al., 1994; Gaskell et al., 2022; see also generally Tindall et al., 2010). It also assumes that the latitudinal gradient in $\delta^{18}O_w$ has not changed through time, which is contradicted by modeling. In warmer climates with an altered hydrological cycle, models predict that regional salinity contrasts should change due to alterations in the local ratio of evaporation to precipitation (Richter and Xie, 2010; Singh et al., 2016), with an analogous effect on $\delta^{18}O_w$ (Zhou et al., 2008; Tindall et al., 2010; Roberts et al., 2011; Zhu et al., 2020). In particularly extreme cases such as the Eocene, the theoretical difference between modern latitude-derived $\delta^{18}O_w$ (after Zachos et al., 1994 Eq. 1) and modeled local $\delta^{18}O_w$ at 6x preindustrial pCO_2 (Zhu et al., 2020) yields a mean temperature error of 5 °C in the Southern Ocean (60–90 °S) or an astonishing mean temperature error of 41 °C above the Arctic Circle (66.5–90 °N; Figure 1).

An alternative approach is to obtain $\delta^{18}O_w$ more or less directly from isotope-enabled climate models (Zhou et al., 2008; Roberts et al., 2011; Gaskell et al., 2022). Several approaches have been adopted: drawing local $\delta^{18}O_w$ directly from model output (Roberts et al., 2011); using modeled zonal mean $\delta^{18}O_w$ for a particular paleolatitude (Zhou et al., 2008); using models as input to fit a generalized equation for predicting $\delta^{18}O_w$ from latitude and bottom-water temperature (Gaskell et al., 2022 Eq. S9); or, recently, a generalized method which uses bottom-water temperature to interpolate local $\delta^{18}O_w$ between models run at different pCO_2 (Gaskell et al., 2022). While some authors have avoided these approaches altogether due to the uncertainty of modeled $\delta^{18}O_w$ (e.g., Hollis et al., 2012) or the possibility of introducing circularity into data-model comparisons (e.g., Hollis et al., 2019), model-derived $\delta^{18}O_w$ clearly captures information lost by simpler approaches and is therefore appropriate for some use-cases (Roberts et al., 2011).

Here, ~~we present~~ a new online tool for $\delta^{18}O$ temperature conversion is presented which automates a range of methods for $\delta^{18}O_w$ reconstruction and correction from the literature, improving the accessibility of advanced methods to workers generating $\delta^{18}O_c$ data. ~~We show that the selection of conversion methodology can have a significant impact on the interpretation of the resulting temperatures, particularly those from warm climate states.~~

2 Description

We present a new online tool for performing $\delta^{18}O_c$-temperature conversions which automates a range of methods from the literature. A preprint version of this tool is available at https://www.danielgaskell.com/d18O *[NOTE: This URL will be updated*

to a permanent institutional URL for publication.] The general workflow for using the tool is summarized in Figure 2; details on the methodology and reasoning behind each option are given below.

2.1 $\delta^{18}O_c$-temperature calibration

After manually entering or uploading a datasheet of $\delta^{18}O_c$ measurements in .csv format, users may select from one of 62 different calibrations from the literature ~~(e.g., Bemis et al., 1998; Kim and O'Neil, 1997; Malevich et al., 2019; Marchitto et al., 2014; etc.)~~(Bemis et al., 1998; Böhm et al., 2000; Bouvier-Soumagnac and Duplessy, 1985; Duplessy et al., 2002; Epstein et al., 1953; Erez and Luz, 1983; Farmer et al., 2007; Geffen, 2012; Godiksen et al., 2010; Grossman and Ku, 1986; Høie et al., 2004; Juillet-Leclerc and Schmidt, 2001; Kim and O'Neil, 1997; Kim et al., 2007; Lynch-Stieglitz et al., 1999; Malevich et al., 2019; Marchitto et al., 2014; McCrea, 1950; Mulitza et al., 2004; O'Neil et al., 1969; Patterson et al., 1993; Reynaud-Vaganay et al., 1999; Rosenheim et al., 2009; Shackleton, 1974; Storm-Suke et al., 2007; Thorrold et al., 1997; Tremaine et al., 2011; White et al., 1999; Willmes et al., 2019). ~~Calibrations are standardized to express $\delta^{18}O_c$ in units of ‰ VPDB and $\delta^{18}O_w$ in units of ‰ VSMOW, following the methods used to construct the original calibrations.~~ All data are expressed with $\delta^{18}O_c$ in units of ‰ VPDB and $\delta^{18}O_w$ in units of ‰ VSMOW, with any standard interconversions expected by the chosen calibration performed automatically. Standard interconversion is notably inconsistent in the literature, with many paleoceanographic papers employing the relationship $\partial^{18}O_{VPDB} = \partial^{18}O_{VSMOW} - 0.27‰$ (Hut, 1987) while many geochemical papers employ the incompatible relationship $\partial^{18}O_{VPDB} = 0.97001\ \partial^{18}O_{VSMOW} - 29.99‰$ (Brand et al., 2014). The former is actually the isotopic offset between the related VPDB-CO_2 and VSMOW-CO_2 scales, but the difference is unimportant so long as all data are treated in the manner the calibration expects, as our tool ensures. Examples of common calibrations and their included standard conversions are given in Table 1.

Where applicable, we use the standardized reformulations of Bemis et al. (1998) and Willmes et al. (2019), or exact algebraic rearrangements of the original equations. For the bayfox core-top calibrations of Malevich et al. (2019), the standard bayfox tool re-fits the calibration coefficients with every run. Since this is computationally expensive, we instead use the linear calibration coefficients fit by runs of bayfoxr 0.0.1 directly in linear functions of the form of Eq. 1 (see Table 1). These yield results equivalent to the full fitting process within numerical error (mean residual = ±0.02 °C, identical to the mean scatter between replicates of the full bayfox fit).

2.2 Global $\delta^{18}O_w$ estimation

Users may ~~then~~ specify global $\delta^{18}O_w$ manually or ~~select one~~choose to draw $\delta^{18}O_w$ by sample age from of 12 different ~~methods or records for estimating~~timeseries of global $\delta^{18}O_w$ from the literature ~~(e.g., Cramer et al., 2011; Miller et al., 2020; Rohling et al., 2021; full list in supplementary material)~~(from Cramer et al., 2011; Henkes et al., 2018; Meckler et al., 2022; Miller et al., 2020; Modestou et al., 2020; Rohling et al., 2021; Veizer and Prokoph, 2015). These records are typically constructed by assuming that the benthic $\delta^{18}O$ record reflects a combination of temperature and ice volume and then subtracting out an independent record of temperature (e.g., using Mg/Ca-based bottom-water temperatures; Cramer et al., 2011) or ice volume

(e.g., using a multi-proxy sea level reconstruction; Rohling et al., 2021) to determine the residual $\delta^{18}O_w$. Which global $\delta^{18}O_w$ record is most realistic remains a contentious topic in the literature, with sea-level and Mg/Ca-based records (e.g., Cramer et al., 2011; Rohling et al., 2021) predicting up to ~1‰ lower $\delta^{18}O_w$ for much of the Cenozoic than records based on clumped isotope paleothermometry (Meckler et al., 2022; see also Agterhuis et al., 2022). We provide both classes of record here for comparison by the user.

Records are mapped to the user data's ages by linear interpolation. The Δ47-based $\delta^{18}O_w$ records of Meckler et al. (2022) included in our tool were generated by interpolating the authors' original results to 0.1 Ma resolution using the Monte Carlo LOESS method and parameters described in the original publication (Meckler et al., 2022).

All built-in $\delta^{18}O_w$ and temperature ~~calibration~~ records are internally converted to four different timescales, so the user can select the timescale consistent with their data: GTS2004 (Gradstein et al., 2005), GTS2012 (Gradstein et al., 2012), GTS2016 (Ogg et al., 2016), and GTS2020 (Gradstein et al., 2020). These timescale conversions are performed by linear interpolation between magnetochron boundaries; dataset files can be found on the project GitHub.

2.3 Local $\delta^{18}O_w$ estimation

The user may ~~then~~ select a method for estimating local $\delta^{18}O_w$. These are as follows: performing no local correction; using modern $\delta^{18}O_w$ from each sample's location and a specified depth (after LeGrande and Schmidt, 2006); using reconstructed Late Holocene or Last Glacial Maximum surface $\delta^{18}O_w$ from each sample's location (model output from Tierney et al., 2020); using $\delta^{18}O_w$ estimated from latitude alone (after Zachos et al., 1994 Eq. 1; or the method of Hollis et al., 2019); using $\delta^{18}O_w$ estimated from latitude and bottom-water temperature (after Gaskell et al., 2022 Eq. S9); or using $\delta^{18}O_w$ estimated from isotope-enabled climate models (GCMs, after the method of Gaskell et al., 2022, presently provided using the datasets of Miocene and Eocene paleogeography used in that publication).

For methods which draw from an existing dataset of $\delta^{18}O_w$, the user may specify a number of degrees latitude/longitude or great-circle radius to average over in order to capture a regional mean when the exact paleocoordinates or local hydrography may not be known. To help determine site locations at the time of deposition, an option is also provided to automatically perform paleocoordinate rotations using the GPlates Web Service (Müller et al., 2018). Ages passed to GPlates are rounded to the nearest 100 ka to reduce the number of API calls.

Our tool does not currently implement any automated consideration of seasonal variation in local $\delta^{18}O_w$, as this is generally treated as negligible by standard methodologies or implicitly baked into the calibration by calibrating against mean annual temperatures and $\delta^{18}O_w$ values (e.g., Malevich et al., 2019).

2.4 Carbonate chemistry effects

Because $\delta^{18}O_c$ is known to vary with aqueous carbonate chemistry (the "carbonate ion effect"; Spero et al., 1997; Bijma et al., 1999; Ziveri et al., 2012), users may also specify a carbonate ion correction factor. This is performed by adjusting $\delta^{18}O_c$ with the linear relationship

$$\delta^{18}O'_c = \delta^{18}O_c - (s[CO_3^{2-}] - 200s), \quad (3)$$

where $\delta^{18}O_c$ is the uncorrected oxygen isotope composition of the carbonate, $\delta^{18}O_c$' is the corrected oxygen isotope composition of the carbonate, s is the selected slope of the effect (in ‰ VPDB per µmol L^{-1} CO_3^{2-}), and $[CO_3^{2-}]$ is the concentration of carbonate ion in solution (in µmol kg^{-1}). This relationship yields no correction when $[CO_3^{2-}]$ = 200 µmol kg^{-1}, an approximation of the mean modern surface value (after the long-term record of Zeebe and Tyrrell, 2019). The user may specify $[CO_3^{2-}]$ manually or select a published long-term record of $[CO_3^{2-}]$ (Tyrrell and Zeebe, 2004; Zeebe and Tyrrell, 2019).

2.5 Tool output

On completion, the tool presents a formatted table of the resulting temperatures, along with any intermediate values (such as estimated $\delta^{18}O_w$) which were required to generate them. Any rows with potential errors (e.g., paleocoordinates which do not yield a valid $\delta^{18}O_w$ estimate or temperatures which exceed the data range of the calibration) are flagged with a warning. For reference, a short summary of methods is also generated, including relevant equations and a complete bibliography of citations in both text and BibTeX formats for the methods employed in each run.

It should be noted that, while the tool automates the process of applying a given calibration method, the user is still responsible for pre-screening their data for diagenetic alteration or other external biases. For example, use of $\delta^{18}O$ data from foraminifera must consider factors such as diagenetic recrystallization, depth habitat, shell size, and the presence of gametogenic calcite (for a review, see Pearson, 2012).

~~3 Demonstration of the effect of $\delta^{18}O_w$ reconstruction methods~~

~~3.1 Data and methods~~

~~To illustrate the effects of differing methods of reconstructing $\delta^{18}O_w$, we apply a range of methods to reported site mean $\delta^{18}O_c$ from planktonic foraminifera in the DeepMIP 0.1 proxy database (Hollis et al., 2019). Because $\delta^{18}O_c$ in planktonic foraminifera is strongly susceptible to diagenetic alteration (Pearson et al., 2001), we use only sites with "glassy" preservation. All temperature conversions are performed using our tool described above, using paleocoordinates reported in the original publication and selecting GTS2012 age datums (Gradstein et al., 2012), the *Orbulina universa* low-light calibration (Bemis et al., 1998), and a global $\delta^{18}O_w$ record based on bottom-water Mg/Ca temperatures (Miller et al., 2020). We do not perform a carbonate ion effect correction due to a lack of data on effect strengths in the Eocene.~~

~~We compare seven methods of estimating local $\delta^{18}O_w$: 1) no correction; 2) the mean modern value over 0–50 m depth (after LeGrande and Schmidt, 2006); 3) the reconstructed surface value at the Last Glacial Maximum (after Tierney et al., 2020); 4) the traditional latitude only method (Zachos et al., 1994 Eq. 1); 5) the updated latitude based method of Hollis et al. (2019); 6) the latitude and bottom water temperature method of Gaskell et al. (2022) Eq. S9; and 7) the climate model based method of Gaskell et al. (2022), with Eocene paleogeography (CESMv1.2 CAM5 model dataset with 1x, 3x, 6x, and 9x preindustrial~~

~~pCO2, after Zhu et al., 2020). Where applicable, mean values are taken from ±5° latitude/longitude around each site's paleocoordinates and bottom-water temperatures are taken from the Mg/Ca-based record of Miller et al. (2020). For PETM intervals, a bottom-water temperature of 17.75 °C (4 °C over latest Paleocene temperatures; Tripati and Elderfield, 2005) is assumed as the full magnitude of warming is not captured in the Miller et al. (2020) temperature record. Note that using Eocene paleocoordinates directly to obtain $\delta^{18}O_w$ estimates from datasets with Quaternary paleogeography (methods #2 and #3) is not strictly appropriate and leads to some sites being omitted due to their paleocoordinates falling over land. In a realistic scenario only methods with appropriate paleogeography should be used.~~

~~For comparison with other proxy estimates, we paired each site with the geographically nearest site (by great circle distance) for which Mg/Ca and TEX_{86} temperature estimates are reported in the DeepMIP v0.1 compilation and then, for each site, calculated the residual between the $\delta^{18}O$-based temperature and the mean of Mg/Ca and TEX_{86} temperatures. Sites lacking matching Mg/Ca and TEX_{86} temperature estimates within a 1650 km radius were omitted, leaving four sites from the North Atlantic: DSDP 401, Bass River, Wilson Lake, and Millville.~~

~~3.2 Results~~

~~Choice of $\delta^{18}O_w$ reconstruction method induces variations in site temperatures with an average standard deviation of 1.5 °C across all sites (i.e., approximately ±3.0 °C error at the 2σ or 95% level). As would be expected from Figure 1, spatially-explicit methods yield higher temperatures than those relying on paleolatitude alone for most sites in the Atlantic, but lower temperatures for sites in the Pacific and Indian Oceans. The updated latitudinal method of Hollis et al. (2019) yields colder temperatures at all sites than the older method of Zachos et al. (1994) Eq. 1, due primarily to differences in predicted Northern Hemisphere $\delta^{18}O_w$. Comparisons between $\delta^{18}O$ based and Mg/Ca+TEX_{86} based temperatures is shown in Figure 3. Using the spatially explicit Gaskell et al. (2022) method produces results that are significantly closer to with Mg/Ca+TEX_{86} based temperatures than the latitudinal method (Hollis et al., 2019) employed by the original DeepMIP v0.1 proxy compilation (F-test of residuals, $p = 0.036$), but are not significantly different from results obtained using the method of Zachos et al. (1994) Eq. 1 ($p = 0.227$).~~

3 Concluding remarks

Our tool provides a convenient way for workers to perform $\delta^{18}O$-temperature conversions and explore the sensitivity of their results to different calibrations, corrections, and $\delta^{18}O_w$-reconstruction methods by successively trying different options in the interface. By allowing data-generators to rapidly generate multiple temperature estimates for their records with different underlying assumptions, our tool allows workers to quickly understand and quantify the effects of different assumptions on the resulting temperature estimates.

~~The demonstration included here suggests that reconstructing $\delta^{18}O_w$ from latitude alone can induce substantial errors and that spatially explicit methods such as that proposed by Gaskell et al. (2022) can significantly improve correspondence between~~

~~$\delta^{18}O$-based temperatures and other proxy estimates, at least in the North Atlantic. However, it should be noted that at high latitudes during the warmest time intervals, $\delta^{18}O$ can yield temperatures 5–10 °C colder than those predicted by other proxies (e.g., Zhu et al., 2019; Gaskell et al., 2022). If models are correct in their predictions that warmer climate states can result in significantly depleted high-latitude $\delta^{18}O_w$ (Zhou et al., 2008; Tindall et al., 2010; Roberts et al., 2011; Zhu et al., 2020), then using model-based methods to reconstruct $\delta^{18}O_w$ would only increase this discrepancy further. Improving our understanding of $\delta^{18}O_w$ changes in warm climate states is therefore an important component of resolving ongoing proxy discrepancies in the high latitudes.~~

Code availability

An online version of the most current release of our tool is maintained at https://www.danielgaskell.com/d18O *[preprint URL, subject to change]*. Source code (Javascript and PHP) is available from the project's GitHub repository at https://github.com/danielgaskell/d18Oconverter.

References

Agterhuis, T., Ziegler, M., de Winter, N. J., and Lourens, L. J.: Warm deep-sea temperatures across Eocene Thermal Maximum 2 from clumped isotope thermometry, Commun Earth Environ, 3, 1–9, https://doi.org/10.1038/s43247-022-00350-8, 2022.

Bemis, B. E., Spero, H. J., Bijma, J., and Lea, D. W.: Reevaluation of the oxygen isotopic composition of planktonic foraminifera: Experimental results and revised paleotemperature equations, Paleoceanography, 13, 150–160, https://doi.org/10.1029/98PA00070, 1998.

Bijma, J., Spero, H. J., and Lea, D. W.: Reassessing Foraminiferal Stable Isotope Geochemistry: Impact of the Oceanic Carbonate System (Experimental Results), in: Use of Proxies in Paleoceanography, edited by: Fischer, D. G. and Wefer, P. D. G., Springer Berlin Heidelberg, 489–512, https://doi.org/10.1007/978-3-642-58646-0_20, 1999.

Böhm, F., Joachimski, M. M., Dullo, W.-C., Eisenhauer, A., Lehnert, H., Reitner, J., and Wörheide, G.: Oxygen isotope fractionation in marine aragonite of coralline sponges, Geochimica et Cosmochimica Acta, 64, 1695–1703, https://doi.org/10.1016/S0016-7037(99)00408-1, 2000.

Bouvier-Soumagnac, Y. and Duplessy, J.-C.: Carbon and oxygen isotopic composition of planktonic foraminifera from laboratory culture, plankton tows and Recent sediment; implications for the reconstruction of paleoclimatic conditions and of the global carbon cycle, Journal of Foraminiferal Research, 15, 302–320, https://doi.org/10.2113/gsjfr.15.4.302, 1985.

Brand, W. A., Coplen, T. B., Vogl, J., Rosner, M., and Prohaska, T.: Assessment of international reference materials for isotope-ratio analysis (IUPAC Technical Report), Pure and Applied Chemistry, 86, 425–467, 2014.

Cramer, B. S., Toggweiler, J. R., Wright, J. D., Katz, M. E., and Miller, K. G.: Ocean overturning since the Late Cretaceous: Inferences from a new benthic foraminiferal isotope compilation, Paleoceanography, 24, PA4216, https://doi.org/10.1029/2008PA001683, 2009.

Cramer, B. S., Miller, K. G., Barrett, P. J., and Wright, J. D.: Late Cretaceous–Neogene trends in deep ocean temperature and continental ice volume: Reconciling records of benthic foraminiferal geochemistry (δ18O and Mg/Ca) with sea level history, Journal of Geophysical Research: Oceans, 116, https://doi.org/10.1029/2011JC007255, 2011.

Duplessy, J.-C., Labeyrie, L., and Waelbroeck, C.: Constraints on the ocean oxygen isotopic enrichment between the Last Glacial Maximum and the Holocene: Paleoceanographic implications, Quaternary Science Reviews, 21, 315–330, https://doi.org/10.1016/S0277-3791(01)00107-X, 2002.

Epstein, S., Buchsbaum, R., Lowenstam, H. A., and Urey, H. C.: Revised carbonate-water isotopic temperature scale, Geological Society of America Bulletin, 64, 1315–1326, 1953.

Erez, J. and Luz, B.: Experimental paleotemperature equation for planktonic foraminifera, Geochimica et Cosmochimica Acta, 47, 1025–1031, https://doi.org/10.1016/0016-7037(83)90232-6, 1983.

Farmer, E. C., Kaplan, A., Menocal, P. B. de, and Lynch-Stieglitz, J.: Corroborating ecological depth preferences of planktonic foraminifera in the tropical Atlantic with the stable oxygen isotope ratios of core top specimens, Paleoceanography, 22, https://doi.org/10.1029/2006PA001361, 2007.

Gaskell, D. E., Huber, M., O'Brien, C. L., Inglis, G. N., Acosta, R. P., Poulsen, C. J., and Hull, P. M.: The latitudinal temperature gradient and its climate dependence as inferred from foraminiferal δ18O over the past 95 million years, Proceedings of the National Academy of Sciences, 119, e2111332119, https://doi.org/doi:10.1073/pnas.2111332119, 2022.

Geffen, A. J.: Otolith oxygen and carbon stable isotopes in wild and laboratory-reared plaice (Pleuronectes platessa), Environ Biol Fish, 95, 419–430, https://doi.org/10.1007/s10641-012-0033-2, 2012.

Godiksen, J. A., Svenning, M.-A., Dempson, J. B., Marttila, M., Storm-Suke, A., and Power, M.: Development of a species-specific fractionation equation for Arctic charr (Salvelinus alpinus (L.)): an experimental approach, Hydrobiologia, 650, 67–77, https://doi.org/10.1007/s10750-009-0056-7, 2010.

Gradstein, F. M., Ogg, J. G., and Smith, A. G. (Eds.): A Geologic Time Scale 2004, Cambridge University Press, Cambridge, https://doi.org/10.1017/CBO9780511536045, 2005.

Gradstein, F. M., Ogg, J. G., Schmitz, M. D., and Ogg, G. M. (Eds.): The Geologic Time Scale, Elsevier, https://doi.org/10.1016/C2011-1-08249-8, 2012.

Gradstein, F. M., Ogg, J. G., Schmitz, M. D., and Ogg, G. M.: Geologic Time Scale 2020, Elsevier, https://doi.org/10.1016/C2020-1-02369-3, 2020.

Grossman, E. L.: Chapter 10 - Oxygen Isotope Stratigraphy, in: The Geologic Time Scale, edited by: Gradstein, F. M., Ogg, J. G., Schmitz, M. D., and Ogg, G. M., Elsevier, Boston, 181–206, https://doi.org/10.1016/B978-0-444-59425-9.00010-X, 2012.

Grossman, E. L. and Ku, T.-L.: Oxygen and carbon isotope fractionation in biogenic aragonite: Temperature effects, Chemical Geology: Isotope Geoscience section, 59, 59–74, https://doi.org/10.1016/0168-9622(86)90057-6, 1986.

Henkes, G. A., Passey, B. H., Grossman, E. L., Shenton, B. J., Yancey, T. E., and Pérez-Huerta, A.: Temperature evolution and the oxygen isotope composition of Phanerozoic oceans from carbonate clumped isotope thermometry, Earth and Planetary Science Letters, 490, 40–50, https://doi.org/10.1016/j.epsl.2018.02.001, 2018.

Høie, H., Otterlei, E., and Folkvord, A.: Temperature-dependent fractionation of stable oxygen isotopes in otoliths of juvenile cod (Gadus morhua L.), ICES Journal of Marine Science, 61, 243–251, https://doi.org/10.1016/j.icesjms.2003.11.006, 2004.

Hollis, C. J., Taylor, K. W. R., Handley, L., Pancost, R. D., Huber, M., Creech, J. B., Hines, B. R., Crouch, E. M., Morgans, H. E. G., Crampton, J. S., Gibbs, S., Pearson, P. N., and Zachos, J. C.: Early Paleogene temperature history of the Southwest Pacific Ocean: Reconciling proxies and models, Earth and Planetary Science Letters, 349–350, 53–66, https://doi.org/10.1016/j.epsl.2012.06.024, 2012.

Hollis, C. J., Dunkley Jones, T., Anagnostou, E., Bijl, P. K., Cramwinckel, M. J., Cui, Y., Dickens, G. R., Edgar, K. M., Eley, Y., Evans, D., Foster, G. L., Frieling, J., Inglis, G. N., Kennedy, E. M., Kozdon, R., Lauretano, V., Lear, C. H., Littler, K., Lourens, L., Meckler, A. N., Naafs, B. D. A., Pälike, H., Pancost, R. D., Pearson, P. N., Röhl, U., Royer, D. L., Salzmann, U., Schubert, B. A., Seebeck, H., Sluijs, A., Speijer, R. P., Stassen, P., Tierney, J., Tripati, A., Wade, B., Westerhold, T., Witkowski, C., Zachos, J. C., Zhang, Y. G., Huber, M., and Lunt, D. J.: The DeepMIP contribution to PMIP4: methodologies for selection, compilation and analysis of latest Paleocene and early Eocene climate proxy data, incorporating version 0.1 of the DeepMIP database, Geoscientific Model Development, 12, 3149–3206, https://doi.org/10.5194/gmd-12-3149-2019, 2019.

Hut, G.: Consultants' group meeting on stable isotope reference samples for geochemical and hydrological investigations, International Atomic Energy Agency, Vienna (Austria), 1987.

Juillet-Leclerc, A. and Schmidt, G.: A calibration of the oxygen isotope paleothermometer of coral aragonite from Porites, Geophysical Research Letters, 28, https://doi.org/10.1029/2000GL012538, 2001.

Kim, S.-T. and O'Neil, J. R.: Equilibrium and nonequilibrium oxygen isotope effects in synthetic carbonates, Geochimica et Cosmochimica Acta, 61, 3461–3475, https://doi.org/10.1016/S0016-7037(97)00169-5, 1997.

Kim, S.-T., O'Neil, J. R., Hillaire-Marcel, C., and Mucci, A.: Oxygen isotope fractionation between synthetic aragonite and water: Influence of temperature and Mg2+ concentration, Geochimica et Cosmochimica Acta, 71, 4704–4715, https://doi.org/10.1016/j.gca.2007.04.019, 2007.

LeGrande, A. N. and Schmidt, G. A.: Global gridded data set of the oxygen isotopic composition in seawater, Geophysical Research Letters, 33, https://doi.org/10.1029/2006GL026011, 2006.

Lynch-Stieglitz, J., Curry, W. B., and Slowey, N.: A geostrophic transport estimate for the Florida Current from the oxygen isotope composition of benthic foraminifera, Paleoceanography, 14, 360–373, https://doi.org/10.1029/1999PA900001, 1999.

Malevich, S. B., Vetter, L., and Tierney, J. E.: Global Core Top Calibration of δ18O in Planktic Foraminifera to Sea Surface Temperature, Paleoceanography and Paleoclimatology, 34, 1292–1315, https://doi.org/10.1029/2019PA003576, 2019.

Marchitto, T. M., Curry, W. B., Lynch-Stieglitz, J., Bryan, S. P., Cobb, K. M., and Lund, D. C.: Improved oxygen isotope temperature calibrations for cosmopolitan benthic foraminifera, Geochimica et Cosmochimica Acta, 130, 1–11, https://doi.org/10.1016/j.gca.2013.12.034, 2014.

McCrea, J. M.: On the Isotopic Chemistry of Carbonates and a Paleotemperature Scale, J. Chem. Phys., 18, 849–857, https://doi.org/10.1063/1.1747785, 1950.

Meckler, A. N., Sexton, P. F., Piasecki, A. M., Leutert, T. J., Marquardt, J., Ziegler, M., Agterhuis, T., Lourens, L. J., Rae, J. W. B., Barnet, J., Tripati, A., and Bernasconi, S. M.: Cenozoic evolution of deep ocean temperature from clumped isotope thermometry, Science, 377, 86–90, https://doi.org/10.1126/science.abk0604, 2022.

Miller, K. G., Browning, J. V., Schmelz, W. J., Kopp, R. E., Mountain, G. S., and Wright, J. D.: Cenozoic sea-level and cryospheric evolution from deep-sea geochemical and continental margin records, Science Advances, 6, eaaz1346, https://doi.org/10.1126/sciadv.aaz1346, 2020.

Modestou, S. E., Leutert, T. J., Fernandez, A., Lear, C. H., and Meckler, A. N.: Warm Middle Miocene Indian Ocean Bottom Water Temperatures: Comparison of Clumped Isotope and Mg/Ca-Based Estimates, Paleoceanography and Paleoclimatology, 35, e2020PA003927, https://doi.org/10.1029/2020PA003927, 2020.

Mulitza, S., Donner, B., Fischer, G., Paul, A., Pätzold, J., Rühlemann, C., and Segl, M.: The South Atlantic Oxygen Isotope Record of Planktic Foraminifera, in: The South Atlantic in the Late Quaternary: Reconstruction of Material Budgets and Current Systems, edited by: Wefer, G., Mulitza, S., and Ratmeyer, V., Springer, Berlin, Heidelberg, 121–142, https://doi.org/10.1007/978-3-642-18917-3_7, 2004.

Müller, R. D., Cannon, J., Qin, X., Watson, R. J., Gurnis, M., Williams, S., Pfaffelmoser, T., Seton, M., Russell, S. H. J., and Zahirovic, S.: GPlates: Building a Virtual Earth Through Deep Time, Geochemistry, Geophysics, Geosystems, 19, 2243–2261, https://doi.org/10.1029/2018GC007584, 2018.

Ogg, J. G., Ogg, G. M., and Gradstein, F. M.: A Concise Geologic Time Scale, Elsevier, https://doi.org/10.1016/C2009-0-64442-1, 2016.

O'Neil, J. R., Clayton, R. N., and Mayeda, T. K.: Oxygen Isotope Fractionation in Divalent Metal Carbonates, J. Chem. Phys., 51, 5547–5558, https://doi.org/10.1063/1.1671982, 1969.

Patterson, W. P., Smith, G. R., and Lohmann, K. C.: Continental Paleothermometry and Seasonality Using the Isotopic Composition of Aragonitic Otoliths of Freshwater Fishes, in: Climate Change in Continental Isotopic Records, American Geophysical Union (AGU), 191–202, https://doi.org/10.1029/GM078p0191, 1993.

Pearson, P. N.: Oxygen Isotopes in Foraminifera: Overview and Historical Review, in: Reconstructing Earth's Deep-Time Climate—The State of the Art in 2012, Paleontological Society Short Course, vol. 18, The Paleontological Society, 1–38, 2012.

Reynaud-Vaganay, S., Gattuso, J.-P., Cuif, J.-P., Jaubert, J., and Juillet-Leclerc, A.: A novel culture technique for scleractinian corals: application to investigate changes in skeletal δ18O as a function of temperature, Marine Ecology Progress Series, 180, 121–130, https://doi.org/10.3354/meps180121, 1999.

Richter, I. and Xie, S.-P.: Moisture transport from the Atlantic to the Pacific basin and its response to North Atlantic cooling and global warming, Clim Dyn, 35, 551–566, https://doi.org/10.1007/s00382-009-0708-3, 2010.

Roberts, C. D., LeGrande, A. N., and Tripati, A. K.: Sensitivity of seawater oxygen isotopes to climatic and tectonic boundary conditions in an early Paleogene simulation with GISS ModelE-R, Paleoceanography, 26, https://doi.org/10.1029/2010PA002025, 2011.

Rohling, E. J.: Oxygen isotope composition of seawater, in: The Encyclopedia of Quaternary Science, Elsevier, Amsterdam, 915–922, 2013.

Rohling, E. J., Yu, J., Heslop, D., Foster, G. L., Opdyke, B., and Roberts, A. P.: Sea level and deep-sea temperature reconstructions suggest quasi-stable states and critical transitions over the past 40 million years, Science Advances, 7, eabf5326, https://doi.org/10.1126/sciadv.abf5326, 2021.

Rosenheim, B. E., Swart, P. K., and Willenz, P.: Calibration of sclerosponge oxygen isotope records to temperature using high-resolution δ18O data, Geochimica et Cosmochimica Acta, 73, 5308–5319, https://doi.org/10.1016/j.gca.2009.05.047, 2009.

Shackleton, N. J.: Attainment of isotopic equilibrium between ocean water and the benthonic foraminifera genus Unigerina : isotopic changes in the ocean during the last glacial., Centre Natl. Rech. Sci. Coll. Inter., 219, 203–209, 1974.

Sharp, Z.: Principles of Stable Isotope Geochemistry, 2nd ed., University of New Mexico Open Textbooks, 416 pp., 2017.

Singh, H. K. A., Donohoe, A., Bitz, C. M., Nusbaumer, J., and Noone, D. C.: Greater aerial moisture transport distances with warming amplify interbasin salinity contrasts, Geophysical Research Letters, 43, 8677–8684, https://doi.org/10.1002/2016GL069796, 2016.

Spero, H. J., Bijma, J., Lea, D. W., and Bemis, B. E.: Effect of seawater carbonate concentration on foraminiferal carbon and oxygen isotopes, Nature, 390, 497–500, https://doi.org/10.1038/37333, 1997.

Storm-Suke, A., Dempson, J. B., Reist, J. D., and Power, M.: A field-derived oxygen isotope fractionation equation for Salvelinus species, Rapid Communications in Mass Spectrometry, 21, 4109–4116, https://doi.org/10.1002/rcm.3320, 2007.

Thorrold, S. R., Campana, S. E., Jones, C. M., and Swart, P. K.: Factors determining δ13C and δ18O fractionation in aragonitic otoliths of marine fish, Geochimica et Cosmochimica Acta, 61, 2909–2919, https://doi.org/10.1016/S0016-7037(97)00141-5, 1997.

Tierney, J. E., Zhu, J., King, J., Malevich, S. B., Hakim, G. J., and Poulsen, C. J.: Glacial cooling and climate sensitivity revisited, Nature, 584, 569–573, https://doi.org/10.1038/s41586-020-2617-x, 2020.

Tindall, J., Flecker, R., Valdes, P., Schmidt, D. N., Markwick, P., and Harris, J.: Modelling the oxygen isotope distribution of ancient seawater using a coupled ocean–atmosphere GCM: Implications for reconstructing early Eocene climate, Earth and Planetary Science Letters, 292, 265–273, https://doi.org/10.1016/j.epsl.2009.12.049, 2010.

Tremaine, D. M., Froelich, P. N., and Wang, Y.: Speleothem calcite farmed in situ: Modern calibration of δ18O and δ13C paleoclimate proxies in a continuously-monitored natural cave system, Geochimica et Cosmochimica Acta, 75, 4929–4950, https://doi.org/10.1016/j.gca.2011.06.005, 2011.

Tyrrell, T. and Zeebe, R. E.: History of carbonate ion concentration over the last 100 million years, Geochimica et Cosmochimica Acta, 68, 3521–3530, https://doi.org/10.1016/j.gca.2004.02.018, 2004.

Veizer, J. and Prokoph, A.: Temperatures and oxygen isotopic composition of Phanerozoic oceans, Earth-Science Reviews, 146, 92–104, https://doi.org/10.1016/j.earscirev.2015.03.008, 2015.

Westerhold, T., Marwan, N., Drury, A. J., Liebrand, D., Agnini, C., Anagnostou, E., Barnet, J. S. K., Bohaty, S. M., Vleeschouwer, D. D., Florindo, F., Frederichs, T., Hodell, D. A., Holbourn, A. E., Kroon, D., Lauretano, V., Littler, K., Lourens, L. J., Lyle, M., Pälike, H., Röhl, U., Tian, J., Wilkens, R. H., Wilson, P. A., and Zachos, J. C.: An astronomically dated record of Earth's climate and its predictability over the last 66 million years, Science, 369, 1383–1387, https://doi.org/10.1126/science.aba6853, 2020.

White, R. M. P., Dennis, P. F., and Atkinson, T. C.: Experimental calibration and field investigation of the oxygen isotopic fractionation between biogenic aragonite and water, Rapid Communications in Mass Spectrometry, 13, 1242–1247, https://doi.org/10.1002/(SICI)1097-0231(19990715)13:13<1242::AID-RCM627>3.0.CO;2-F, 1999.

Willmes, M., Lewis, L. S., Davis, B. E., Loiselle, L., James, H. F., Denny, C., Baxter, R., Conrad, J. L., Fangue, N. A., Hung, T.-C., Armstrong, R. A., Williams, I. S., Holden, P., and Hobbs, J. A.: Calibrating temperature reconstructions from fish otolith oxygen isotope analysis for California's critically endangered Delta Smelt, Rapid Communications in Mass Spectrometry, 33, 1207–1220, https://doi.org/10.1002/rcm.8464, 2019.

Zachos, J., Pagani, M., Sloan, L., Thomas, E., and Billups, K.: Trends, Rhythms, and Aberrations in Global Climate 65 Ma to Present, Science, 292, 686–693, https://doi.org/10.1126/science.1059412, 2001.

Zachos, J. C., Stott, L. D., and Lohmann, K. C.: Evolution of Early Cenozoic marine temperatures, Paleoceanography, 9, 353–387, https://doi.org/10.1029/93PA03266, 1994.

Zeebe, R. E. and Tyrrell, T.: History of carbonate ion concentration over the last 100 million years II: Revised calculations and new data, Geochimica et Cosmochimica Acta, https://doi.org/10.1016/j.gca.2019.02.041, 2019.

Zhou, J., Poulsen, C. J., Pollard, D., and White, T. S.: Simulation of modern and middle Cretaceous marine δ18O with an ocean-atmosphere general circulation model, Paleoceanography, 23, https://doi.org/10.1029/2008PA001596, 2008.

Zhu, J., Poulsen, C. J., Otto-Bliesner, B. L., Liu, Z., Brady, E. C., and Noone, D. C.: Simulation of early Eocene water isotopes using an Earth system model and its implication for past climate reconstruction, Earth and Planetary Science Letters, 537, 116164, https://doi.org/10.1016/j.epsl.2020.116164, 2020.

Ziveri, P., Thoms, S., Probert, I., Geisen, M., and Langer, G.: A universal carbonate ion effect on stable oxygen isotope ratios in unicellular planktonic calcifying organisms, Biogeosciences, 9, 1025–1032, https://doi.org/10.5194/bg-9-1025-2012, 2012.

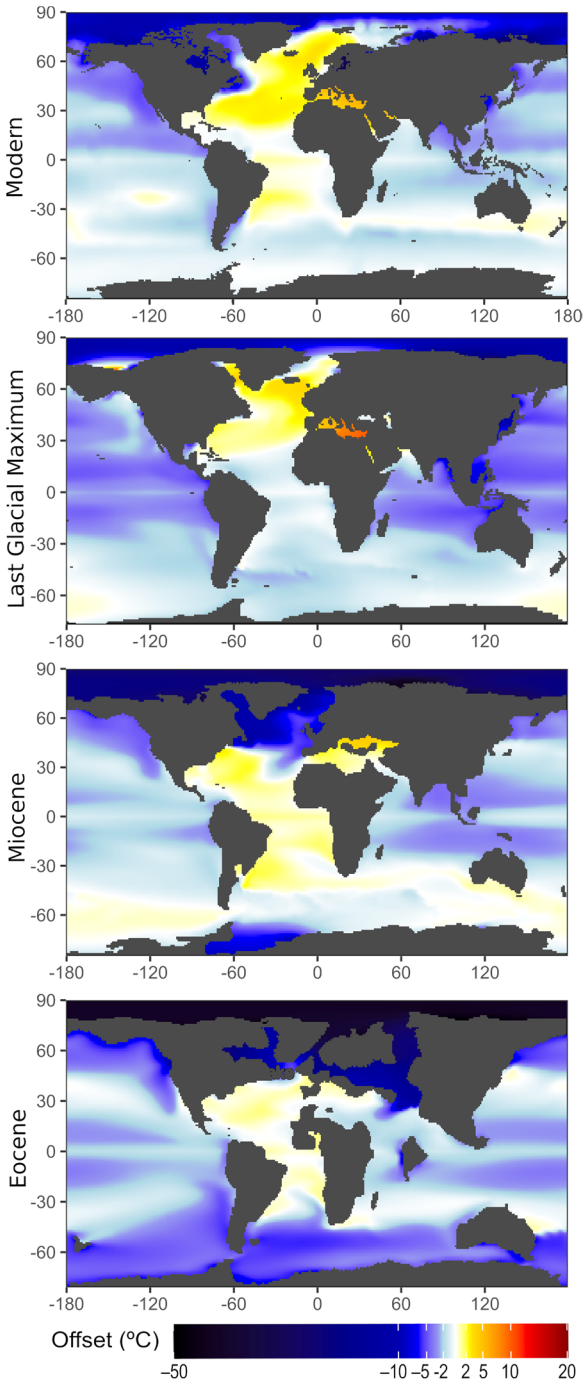

Figure 1: Effect of estimating SST using measured/modelled local $\delta^{18}O_w$ rather than the latitude-based approximation of Zachos et al. (1994) Eq. 1. Modern: comparison with mean annual $\delta^{18}O_w$ <50 m depth (after LeGrande and Schmidt, 2006). Last Glacial Maximum (LGM): comparison with inferred annual surface $\delta^{18}O_w$ at the LGM (Tierney et al., 2020). Miocene: comparison with CESMv1.2_CAM5 model run at 400 ppm CO_2 with Miocene paleogeography (Gaskell et al., 2022). Eocene: comparison with CESM_1.2_CAM5 model run at 6x preindustrial CO_2 with Eocene paleogeography (Zhu et al., 2020). Temperatures are calculated assuming a slope of 4.80 °C ‰$^{-1}$ (Bemis et al., 1998).

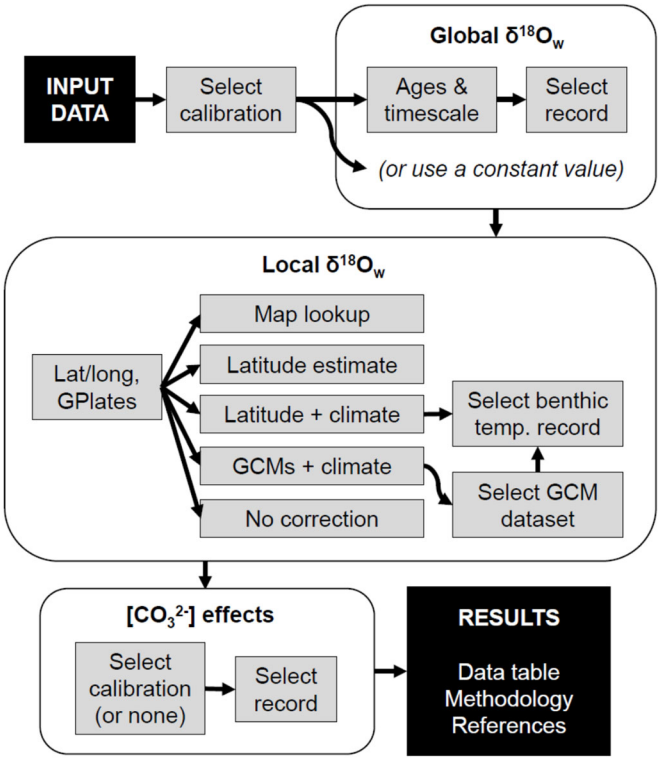

385

Figure 2: General workflow for using the tool. (Each box may reflect multiple sub-options.)

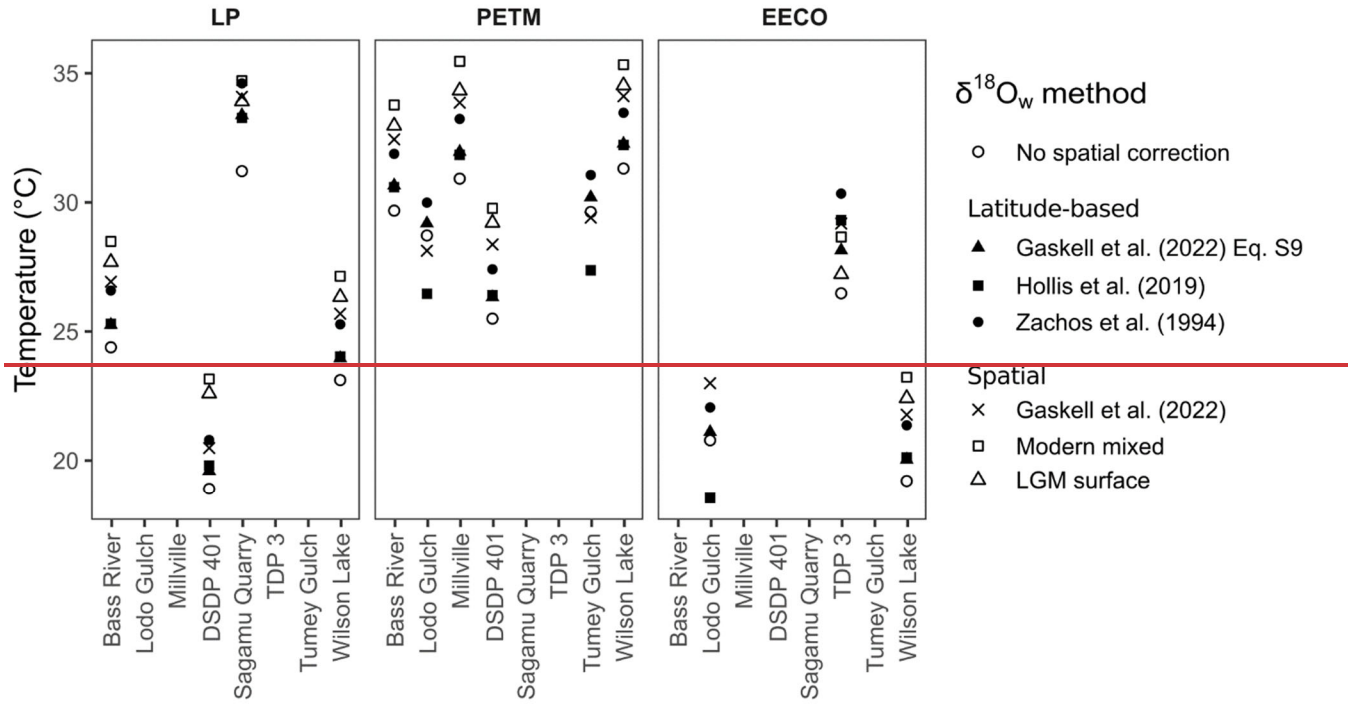

Figure 2: DeepMIP v0.1 $\delta^{18}O$ sites converted to temperature after the seven methods described in the text. Age groupings follow the original publication (LP = Latest Paleocene, PETM = Paleocene-Eocene Thermal Maximum, EECO = Early Eocene Climate Optimum; Hollis et al., 2019).

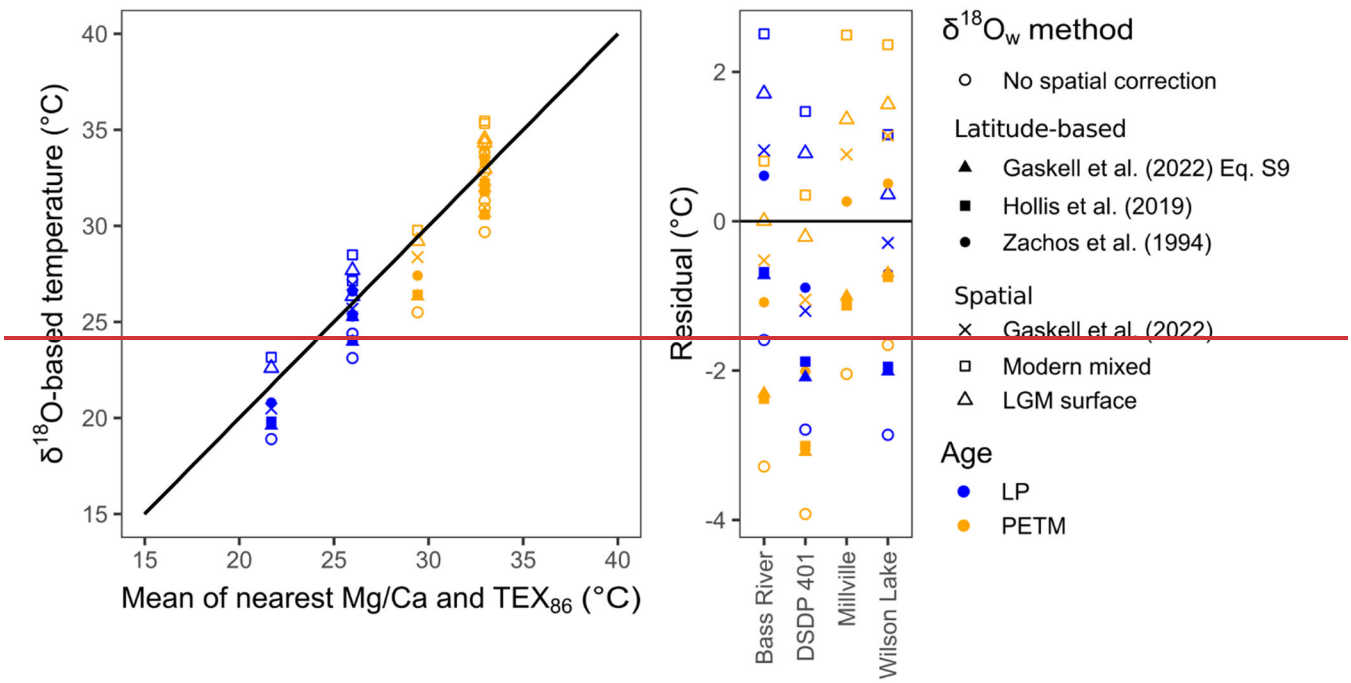

395 **~~Figure 3: Comparison of $\delta^{18}O$-based temperatures with the mean of the geographically nearest Mg/Ca and TEX_{86}-based temperatures from the DeepMIP v0.1 proxy compilation.~~**

Table 1: Commonly applied $\delta^{18}O$:temperature calibrations from the literature. The tool includes a total of 62 calibrations, which are cited above and listed in the tool interface. Full algebraic rearrangements used by the tool are available in the source code on GitHub. $\Delta^{18}O_c = \partial^{18}O_c - \partial^{18}O_w$, where the given VSMOW conversion factor is first added to $\partial^{18}O_w$ to convert VSMOW into the format expected by the calibration.

Reference	Material	Method	Equation	VSMOW to VPDB	Bounds (°C)	Typical application
(Kim and O'Neil, 1997)	Inorganic calcite	Laboratory precipitation	$T = 16.1 - 4.64\,\Delta^{18}O_c + 0.09\,(\Delta^{18}O_c)^2$	−0.27‰*	0–40	"Equilibrium calcite" temperatures, e.g., inferring calcification depth from $\delta^{18}O_c$
(Kim et al., 2007)	Inorganic aragonite	Laboratory precipitation	$T = \frac{17.88 \times 10^3}{1000 \ln\left(\frac{\partial^{18}O_c + 29.99}{\frac{0.97001}{\partial^{18}O_w + 1000}} + 1000\right) + 31.14} - 273.15$	0‰†	0–40	"Equilibrium aragonite" temperatures
(Malevich et al., 2019)	Planktonic foraminifera	Core-top regression	Several Bayesian fits; 50% quantile temperatures for the annual multi-species pooled method follow the relationship: $T = 11.8790 - 4.0562\,\Delta^{18}O_c$	0‰‡	0–29.5	Sea-surface temperatures (SSTs)
(Bemis et al., 1998)	*Orbulina universa*	Culture experiment	Mean of high-light and low-light calibrations: $T = 15.7 - 4.80\,\Delta^{18}O_c$	−0.27‰§	15–25	Mixed-layer temperatures experienced by photosymbiotic planktonic foraminifera
(Marchitto et al., 2014)	*Cibicidoides* and *Planulina*	Core-top regression	$T = \frac{0.245 - \sqrt{0.045461 + 0.0044\,\Delta^{18}O_c}}{0.0022}$	0‰	–0.6–25.6	Bottom-water temperatures experienced by epifaunal benthic foraminifera
(Marchitto et al., 2014)	*Uvigerina peregrina*	Core-top regression	Recommended method: subtract 0.47‰ from $\delta^{18}O_c$ and use *Cibicidoides* eq. above	n/a	n/a	Bottom-water temperatures experienced by infaunal benthic foraminifera
Other notable historical calibrations						
(Epstein et al., 1953)	Biogenic carbonates	Modern specimens	$T = 16.5 - 4.30\,\Delta^{18}O_c + 0.14\,(\Delta^{18}O_c)^2$	−0.27‰‖	7–30	Temperatures experiences by mollusks and other generic biocalcifiers
(Shackleton, 1974)	*Uvigerina* spp.	Core-top regression	$T = 16.9 - 4.0\,\Delta^{18}O_c$	−0.20‰*	0.8–7	Bottom-water temperatures experienced by infaunal benthic foraminifera
(Erez and Luz, 1983)	*Trilobatus sacculifer*	Culture experiment	$T = 17.0 - 4.52\,\Delta^{18}O_c + 0.03\,(\Delta^{18}O_c)^2$	−0.22‰*	14–30	Mixed-layer temperatures experienced by photosymbiotic planktonic foraminifera

*Reformulated by Bemis et al. (1998)

†Rearranged by this work; the relationship $\partial^{18}O_{VPDB} = 0.97001\,\partial^{18}O_{VSMOW} - 29.99$ (Brand et al., 2014) is included in this equation to convert $\delta^{18}O_c$ from VPDB to VSMOW, as required by the calibration, and temperature has been converted from Kelvin to °C

‡Reformulated in this work by extracting the linear coefficients from the Bayesian posterior values

§Rearranged by this work

‖Reformulated by Bemis et al. (1998) (with VSMOW correction after Grossman, 2012)